Bio-based Scaffolds for Bone Tissue Regeneration

Adam Aberra Challa, Ph.D.

Doctoral Thesis Summary

Tomas Bata University in Zlín

Tomas Bata University in Zlín
Centre of Polymer Systems

Doctoral Thesis Summary

Bio-based Scaffolds for Bone Tissue Regeneration

Biologické Scaffoldy pro Regeneraci Kostní Tkáně

Author:	**Adam Aberra Challa, Ph.D.**
Degree programme:	P0711D130024 Biomaterials and Biocomposites
Supervisor:	doc. Nabanita Saha, M.Sc, Ph.D.
Consultant:	prof. Ing. Petr Sáha, CSc., dr. h. c.
Reviewers:	Prof. Ing. Otakar Bokůvka, Ph.D.
	Adjunct prof. Ing. Natalia Kazantseva, CSc.

Zlin, September 2025

Published by **Tomas Bata University in Zlín** in the Edition **Doctoral Thesis Summary.**

The publication was issued in the year 2025

Klíčová slova *Udržitelné biomateriály, Konstrukce scaffold, Biokompatibilita, Bakteriální celulóza, Oxid grafenu, Hydroxyapatit, Výpočetní analýza*

Keywords: *Sustainable biomaterials, Scaffold design, Biocompatibility, Bacterial cellulose, Graphene oxide, Hydroxyapatite, Computational analysis*

Full text of the doctoral thesis is available in the Library of TBU in Zlín.

ISBN 978-80-7678-361-4

ACKNOWLEDGMENT

This thesis work became a fruit through the help, participation, and immense support of multiple parties. I would like to start my gratitude by acknowledging the Ministry of Education, Youth and Sports of the Czech Republic, which financed my PhD study through the Czech Government Scholarship available to countries including Ethiopia. I would not be here if it were not for the opportunity it provided. I would then like to thank my supervisor doc. Nabanita Saha for all the guidance and counseling she provided me through my 4 years at Tomas Bata University (TBU) in Zlin. This extends to my consultant prof. Ing. Petr Saha who believed in me in the first place and facilitated my smooth study and research in the Center of Polymer Systems (CPS). My former colleague Fahanwi Asabuwa Ngwabebhoh was instrumental in getting me situated in my working space and showed me several ways to succeed. My day-to-day colleagues Oyunchimeg Zandraa and Mainak Chaudhuri helped me a lot in all of my research activities. Thus, I am very grateful to my small research community.

It is not easy to maneuver the world of academics at this stage alone. One needs a strong backbone, or a means of reliance. My dear wife Ada Ioana Barbu has been both. I have deep gratitude. This also extends to my dear friend Sandeep Kumar Dey who crossed paths to show me how to be confident in my journey. I am very thankful to my brothers Leul Aberra and Amanuel Aberra, who have been there for me in all times of need and helped me make the Czech Republic my home. It is also through the persistent check-up and support of my whole family back in Ethiopia that I was able to navigate through tough times in my study stay, hence I am indebted to them as well. I am also grateful to Michal Studeny and Patrik Foltyn who were always available for immediate assistance whenever I felt overwhelmed by official matters.

Last but not least, I would like to appreciate the whole academia of CPS for all the camaraderie from which I benefited, whether it was in terms of scientific help or directional assistance. The rest is my ultimate gratitude to God, who said no to my weaknesses and showed me the way to cross the finish line.

DEDICATION

I dedicate this work to the person who sacrificed a lot to see me fulfilled and happy; my mother, Elizabeth Berhe.

RESUME

Tato práce představuje komplexní studii struktury kostí a mechanismů hojení zlomenin se zaměřením na návrh scaffold v kontextu regenerace tkání. Regenerace kosti s kritickými defekty vyžaduje složité procesy, jako je roubování, k dosažení původní formy. Tkáňové inženýrství kostí se stalo slibným řešením a pro podporu hojení kostí jsou vyvíjeny biokompatibilní scaffold. Scaffold poskytují platformu pro buněčné připojení, proliferaci a diferenciaci. Tato studie zkoumá klíčové aspekty návrhu scaffold, včetně požadavků na výkon, výběru biomateriálů a technologií výroby. Experimentální práce zahrnuje syntézu a charakterizaci biokompozitních scaffold odvozených z bakteriální celulózy (BC), oxidu grafenu (GO), acetátu celulózy (CA) a hydroxyapatitu (HAp). Tyto biomateriály byly vybrány pro své jedinečné a doplňkové vlastnosti se zaměřením na udržitelnost – většina z nich byla odvozena z potravinového odpadu a syntetizována za použití nízkoenergetických procesů, kde je to možné. K výrobě scaffold, která vykazují vlastnosti vhodné pro regeneraci kostí, byly použity různé techniky. SEM odhalil nanovlákennou architekturu BC, která přispívá k jeho strukturálním charakteristikám. FTIR spektroskopie potvrdila přítomnost funkčních skupin obsahujících kyslík v GO, zatímco EDX analýza ukázala, že poměr Ca/P syntetizovaného HAp se blíží stechiometrické hodnotě. Pokud jde o biokompozity, in situ růst hydrogelu prokázal biokompatibilní povahu BC; GO zvýšil pevnost v tahu elektrostaticky zvlákněných CA vláken; a začlenění částic HAp zvýšilo bioaktivitu a osteokonduktivní potenciál scaffold. Dále byly provedeny numerické výpočty za účelem analýzy strukturálního chování teoretického návrhu scaffold při předpokládaném zatížení a modifikace jeho struktury pro požadovaný výstup.

Klíčová slova: *Udržitelné biomateriály, Konstrukce scaffold, Biokompatibilita, Bakteriální celulóza, Oxid grafenu, Hydroxyapatit, Výpočetní analýza*

SUMMARY

This thesis presents a comprehensive study of bone structure and fracture healing mechanisms, focusing on scaffold design within the context of tissue regeneration. Regeneration of bone with critical defects requires complex processes, such as grafting, to obtain the original form. Bone tissue engineering has become a promising solution for developing biocompatible scaffolds to promote bone healing. The scaffolds provide a platform for cellular attachment, proliferation, and differentiation. This study explores key aspects of scaffold design, including performance requirements, biomaterial selection, and fabrication technologies. The experimental work involves the synthesis and characterization of biocomposite scaffolds derived from bacterial cellulose (BC), graphene oxide (GO), cellulose acetate (CA), and hydroxyapatite (HAp). These biomaterials were chosen for their unique and complementary properties, with a focus on sustainability—most were derived from food waste and synthesized using low-energy processes where possible. Different techniques were utilized to fabricate scaffolds that demonstrate properties suitable for bone regeneration. SEM revealed the nanofibrous architecture of BC, which contributes to its structural characteristics. FTIR spectroscopy confirmed the presence of oxygen-containing functional groups in GO, while EDX analysis showed the Ca/P ratio of the synthesized HAp to be close to the stoichiometric value. Regarding the biocomposites, in situ growth of hydrogel showed the biocompatible nature of BC; GO enhanced the tensile strength of electrospun CA fibers; and the incorporation of HAp particles increased the bioactivity and osteoconductive potential of the scaffolds. Additionally, numerical computation was conducted to analyze the structural behavior of a theoretical scaffold design under predicted loading and to modify its structure for a desired output.

Keywords: *Sustainable biomaterials, Scaffold design, Biocompatibility, Bacterial cellulose, Graphene oxide, Hydroxyapatite, Computational analysis*

CONTENTS

1. INTRODUCTION

Bone tissue regeneration (BTR) is the concept of healing a damaged bone using engineered biomaterials. These biomaterials are designed and fabricated in a process known as bone tissue engineering (BTE), one segment of tissue engineering whereby biological elements are fabricated to repair or reconstruct bone tissues and cellular products [1]. It is a multidisciplinary field that encompasses a wide variety of concepts. It integrates the principles of materials science, physical and chemical sciences, engineering, biomedicine, and clinical research to create functional scaffolds for bone regeneration.

To discuss about essence of BTR, it is essential to state the composition and properties of bone first. Bone has a complex, layered, and compartmentalized architecture, as it is evident in Fig. 1.1. Bone's profile is classified as cortical (compact) and cancellous (spongy) bone. Cortical bone constitutes the wall of the tubular shaft of a long bone known as the diaphysis. In its layer called periosteum, an interplay between osteoblasts, osteocytes, osteoclasts, other bone cells, and matrix takes place. Whereas the cancellous bone is the hierarchical, porous bone that is found in the epiphysis and metaphysis of long bones [2]. The osteons that make up this part of the bone also house bone cells and bone matrix.

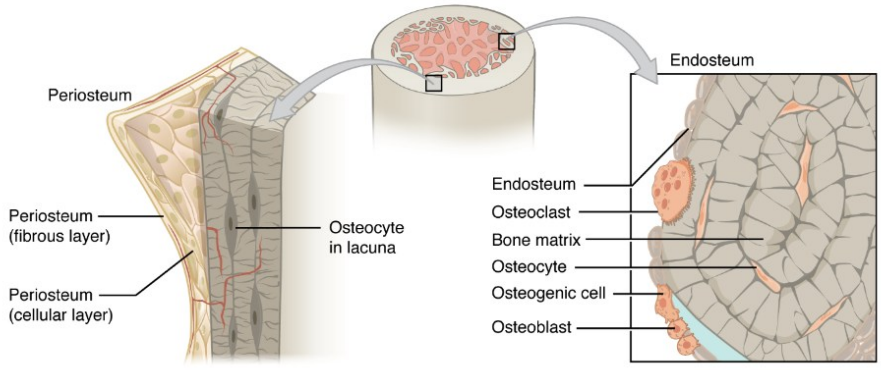

Figure 1.1: The essential classification of bone. The layered structure containing the periosteum and endosteum [3]

Osteogenesis, the bone-forming process, is an interesting phenomenon. Bone progenitor cells, known as pre-osteoblasts, are found in the periosteum and endosteum. They are derived from mesenchymal stem cells (MSCs) and differentiate into osteoblasts with the help of growth factors such as bone morphogenetic proteins

(BMPs) and transforming growth factor-β (TGF-β) [4]. These bone cells grow and mature through crosslinking of proteins and formation of collagen as bone matrix, becoming osteocytes [5]. On the other hand, when it is time, osteoclasts resorb parts of the bone by first embedding themselves to the surface and then creating an acidic environment that dissolves bone mineral and degrades its organic matrix [6].

Bone is a composite structure by nature. It mainly consists of proteins (out of which collagen is the most abundant) (30%), bone mineral (60%), and water (10%) [7]. The collagen fibers (mainly type 1 collagen) constitute the organic bone matrix. Whereas the bone mineral is the inorganic part of the matrix and is mainly composed of hydroxyapatite (HAp) crystals. These crystals are calcium phosphate minerals with a chemical formula of $Ca_{10}(PO_4)_6(OH)_2$[8]. The former serves as a scaffolding for the crystals to grow on and calcify/mineralize [9, 10]. Through these mineralization processes, the HAp gives the bone its hardness. In essence, collagen provides elasticity to bone, and its fibers reinforce HAp crystals, denoting that bone functions as a structural composite.

Due to its stiff structure, owing to the presence of the lamellae and surrounding cement lines, the cortical/compact bone can withstand a larger stress both in tension and compression. The difference between the mechanical performance of cortical and trabecular bone is given in Table 1.1 below.

Table 1.1: Mechanical properties of parts of bone [11, 12]

Components	**Compressive strength (MPa)**	**Tensile strength (MPa)**	**Young's modulus (GPa)**
Cortical bone	100-200	50-150	7-30
Cancellous bone	2-20	10-20	0.1-2

Bone also possesses other excellent features in its mechanical form. Although it is considered a brittle material, it has a commendable toughness. For instance, its fracture energy (G_c) measures 1.5kJ/m^2, which is parallel to that of steel at low temperatures and of wood when measured in alignment to its grain [13].

When bone health is not maintained, however, either in the absence of the above functionalities or due to diseases, bone trauma occurs. The following chapter discusses bone damage, healing mechanisms, and trends in regeneration through BTE.

2. CURRENT STATE OF TOPIC

Bone injury is an increasingly common global health issue. Globally, over 178 million bone fractures occur every year, according to a study made in 2019 [14]. This number was projected to increase every year. The causes can vary from accidents to infections and bone diseases. For a limited injury, bone can heal itself through the integrated work of its cells. The regeneration process has four distinctive steps: hematoma formation, soft callus formation, resorption of soft callus to form hard callus, and lastly bone remodeling (Fig. 2.1). These steps encompass various aspects of bone functions. Stem cells differentiate into fibroblasts, osteoblasts, and chondroblasts [15]. Ossification takes place to construct a layered woven bone. The angiogenesis process then follows with the involvement of growth factors. Finally, osteoblasts deposit new bone, which hardens through time to complete the cycle [16].

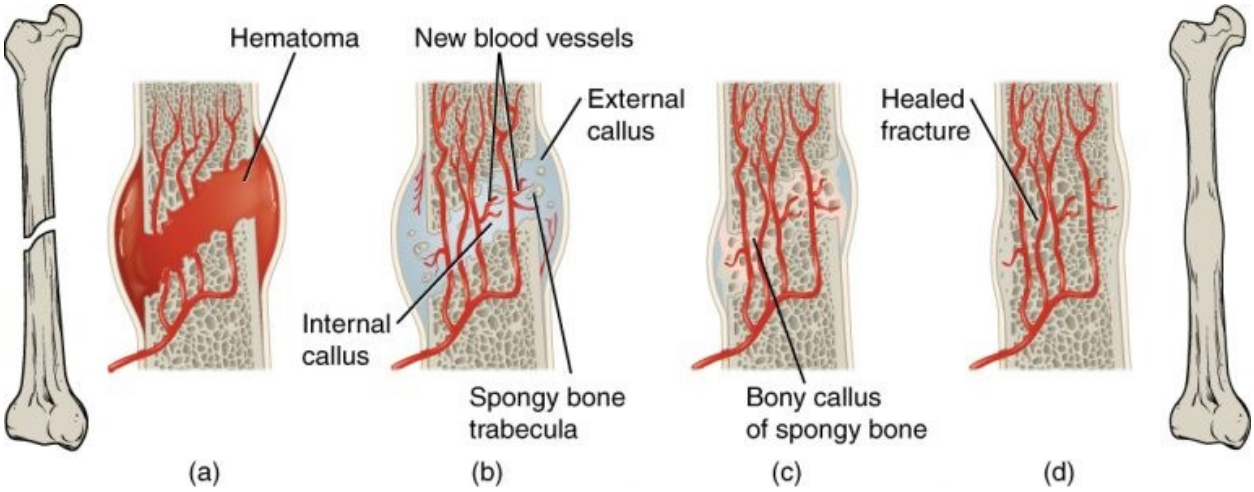

Figure 2.1: Bone remodeling process from fracture to healing [3]

If the damage to the bone is beyond a certain limit, however, i.e. a critical defect, a fracture gap greater than 2-2.5 cm [17], it needs an external intervention for the tissues to regenerate. This is through grafting, mainly classified as autograft, allograft, and xenograft [18]. However, these methods present challenges in terms of immunology, donor site rejection, and the need for additional surgery [19].

BTE presents an alternative to the conventional practices mentioned above with the introduction of scaffolds. Suitable scaffolds are fabricated from biomaterials. Stem cells are seeded onto their surfaces under growth medium. Then, the enriched scaffolds are implanted into the required site. The following sections discuss the ideal requirements, types of materials used, and methods of fabrication of scaffolds.

3. THEORETICAL BACKGROUND

In order to achieve the desired result, a scaffold needs to qualify for several requirements. The more requirements fulfilled, the greater the success of its regenerative capacity. Several of the anticipated properties are discussed below.

3.1. Properties of an ideal scaffold for BTR

Porosity: A 3D porous structure is required to enable cell proliferation and migration, as well as the transport of nutrients throughout a scaffold. A scaffold with smaller porosity (less than 100 μm) shows better cell attachment due to the high available surface area [20]. In the case of diffusion of fluids within the matrix, however, larger pore sizes are essential.

Biodegradability: After implantation, a scaffold must gradually degrade to make way for new bone formation. This process requires for the scaffold to degrade at a rate that matches bone growth under the physiological and microfluidic conditions of the application site. A controlled, gradual degradation is crucial to ensure effective load transfer from the scaffold to the newly forming tissue [21].

Mechanical strength: A scaffold is expected to match the mechanical performance of native bone tissues. As a tissue growth platform, its strength and stiffness profile, including Young's modulus, compressive, and tensile stress, needs to sustain the required value until it degrades. In addition, the scaffold's stiffness plays a role in regulating cell adhesion and proliferation [22].

Biocompatibility: Since a scaffold is fabricated to assimilate with the conditions in the human body, it is expected to pose no harm to the internal mechanisms. It is required to have a positive interaction with the surrounding tissues and new tissues being formed. This is explained by having none to very low cytotoxicity and inflammatory response, promoting cell attachment and growth, and positively facilitating the regeneration of tissues[12].

Osteoconduction and osteoinduction: Osteoconductivity is a property of a scaffold to promote adhesion and growth of bone cells or osteoblasts on its surface through its porous microarchitecture [23]. Whereas the ability of the scaffold to induce bone formation by recruitment of progenitor cells and stimulating them to form preosteoblasts is termed as osteoinductivity [24].

3.2. Materials used in BTR

A wide range of materials can be utilized to fabricate scaffolds for BTR. Broadly categorized into metals, ceramics, polymers, and composites, each offers distinct advantages tailored to specific clinical, biological, and mechanical requirements.

Metals: Titanium, cobalt, aluminum, zirconium, stainless steel, and their alloys have been extensively used as scaffolds in hard tissue regeneration and as load-bearing implants in parts such as the knee and hip joints [25].. However, their potential release of toxic ions, non-resorbability, and inability to induce osseointegration are their major drawbacks [26].

Ceramics: Highly favored because of their biocompatibility due to their chemical similarity to bone's composition. Calcium phosphate ceramics, including hydroxyapatite and tricalcium phosphate, are widely regarded as biomimetic substitutes. In addition, materials such as bioactive glasses**,** magnesium phosphates, and calcium-based salts have shown potential to enhance osteogenic responses [16].

Polymers: Natural polymers, high in molecular weight and excellent in cell-material interactions, include collagen, gelatin, silk fibroin, chitosan, and bacterial cellulose [27, 28]. Selected polymers are discussed in Table 3.1 below. Synthetic polymers include polycaprolactone (PCL), polyethylene glycol (PEG), polylactic acid (PLA), and polyglycolic acid (PGA) [29]. Their rate of degradation can be tailored to regulate the rate of tissue regeneration by adjusting their chemical composition.

Table 3.1: Natural polymers used in BTE and their attributes [30-33]

Polymer	Molecular structure	Synthesis	Disadvantage	Advantage
Bacterial cellulose	Linear polysaccharide, made from β-D-glucopyranose units	Produced from various bacterial strains	Low porosity, slow biodegradation	Biocompatibility, hydrophilicity, easy to obtain
Collagen	Fibrous protein, with a helix structure of amino acids	Extracted from mammalian's connective tissue	Poor antigenicity, requires tissues from animals	Similarity to natural ECM of native tissues
Alginate	Linear polysaccharide, made of β-D-mannuronic acid	Produced from brown algae and seaweeds	Minimal cell-material interaction	Biocompatibility, ability to achieve gelation
Chitosan	Linear polysaccharide made of D-glucosamine	Synthesized from the shells of crustaceans	Low mechanical strength and stability	Antibacterial property, biodegradability

The following subsection discusses the properties and applications of the biomaterials that were chosen as subjects in this study.

3.2.1. Bacterial cellulose

Bacterial cellulose (BC) is a cellulose biopolymer synthesized by various bacterial strains such as *Komagataeibacter*, *Acetobacter*, *Azotobacter*, and *Rhizobium* [34]. Because it is free of hemicellulose and lignin impurities, it has a high crystallinity with other functionalities. BC features a thin fibrous network composed of β-D-glucopyranose units that are linked by β-1,4 glycosidic bonds. This nanofibril network of BC gives rise to its high surface area and porosity. At the molecular level, as shown in Fig. 3.1 below, the cellulose chains in the biopolymer network contain a high density of hydroxyl groups. Its favorable structure makes it ideal for cell growth and propagation, a necessary attribute for a good tissue scaffold [35].

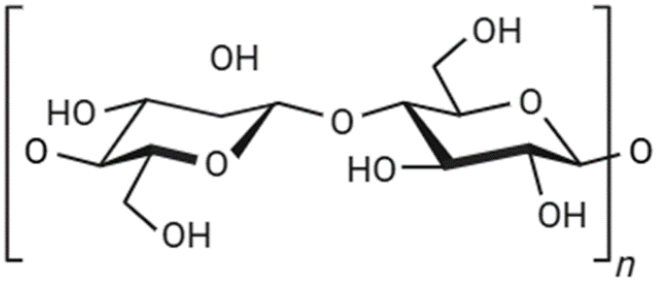

Figure 3.1: Chemical structure of BC [36]

3.2.2. Graphene oxide

Graphene oxide (GO) is an oxidized form of graphene, produced by the intercalation and chemical oxidation of graphite. Its most widely used synthesis approach is the modified Hummers' method [37, 38], where a strong acid is used as an intercalation agent between the graphite layers, and an oxidizing agent is used to create its oxygen groups. Its structure, as shown in Fig. 3.2 below, is enriched with various oxygen-containing functional groups. These include carboxyl (–COOH), epoxy (C–O–C), hydroxyl (–OH), and carbonyl (C=O) [39], which amplify the hydrophilicity of GO.

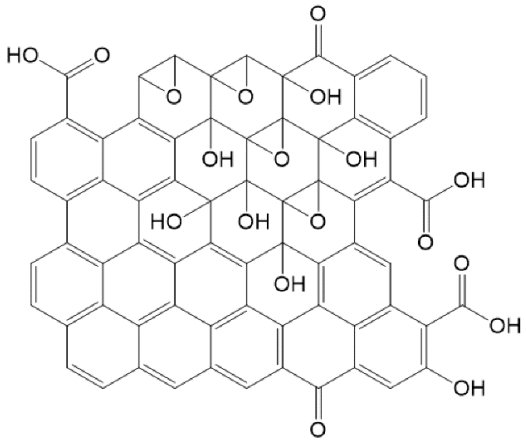

Figure 3.2: Chemical structure of GO (Lerf–Klinowski model) [40]

3.2.3. Cellulose acetate

Cellulose acetate (CA), with a chemical structure shown in Fig. 3.3 below, is a naturally derived biopolymer widely recognized for its excellent biocompatibility, non-toxicity, and renewability. Hence, CA has been extensively explored for

biomedical applications, particularly in tissue engineering. It has demonstrated the ability to support osteoblast proliferation and promote osteogenic differentiation, highlighting its potential in bone regeneration [41]. However, despite these biological advantages and its ease of processing, pristine CA suffers from inherently low mechanical strength, limiting its applicability in tissue engineering [42]. This necessitates the development of CA-based biocomposites.

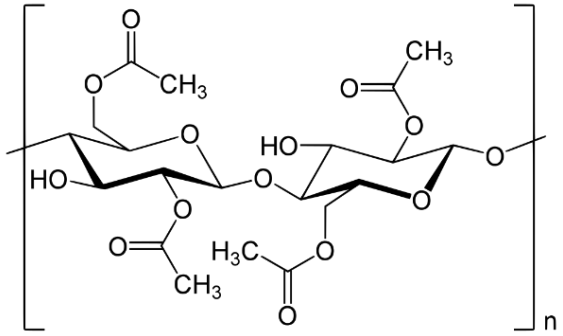

Figure 3.3: Chemical structure of CA [43]

3.2.4. Hydroxyapatite

Hydroxyapatite (HAp; $Ca_{10}(PO_4)_6(OH)_2$) is a naturally occurring calcium phosphate mineral and the primary inorganic component of vertebrate bone, comprising approximately 60–70% of its total weight. Its Ca-P bonds are shown in Fig. 3.4 below. As discussed in the Introduction, HAp belongs to the apatite group of minerals and plays a critical role in the structural and functional integrity of bone tissues. It is widely recognized for its excellent biocompatibility, bioactivity, and osteoconductive capabilities [44].

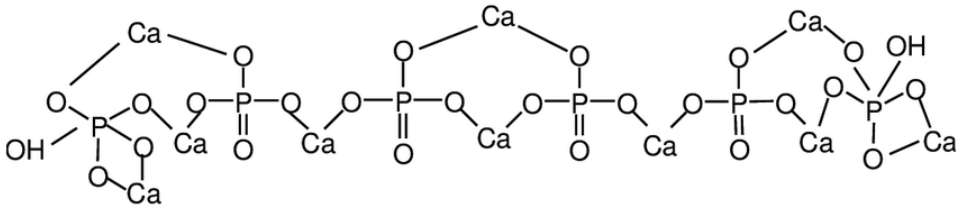

Figure 3.4: Chemical structure of HAp [45]

3.2.5. Composites

Composite biomaterials offer the advantage of possessing the beneficial properties of different classes of materials while mitigating their limitations. Various merits can be achieved through composite formation, such as enhancing the bioactivity of

metallic scaffolds or reinforcing polymers. For instance, calcium phosphate coatings on bioglass, metals, and synthetic polymers have been found to promote cell proliferation and osteoconductivity. Additionally, the addition of natural polymers into scaffold structures has been proven to enhance mineralization and alkaline phosphatase synthesis [46].

3.3. Methods for scaffold fabrication

There are various techniques to synthesize biomaterials and fabricate scaffolds for BTR. The choice is highly dependent on the behavior of the source materials, the target output, and the intended application. Some of the main techniques are described below.

Sol-gel technology: Inorganic salts or metal-organic compounds are dissolved in a suitable solvent, initiating polymerization reactions that lead to the formation of a colloidal suspension [47]. When this suspension (sol) is cast into a mold, it undergoes gelation, resulting in the formation of a wet gel. Subsequent drying transforms the gel into a dense ceramic or glass material. This technique is considered beneficial because it results in high chemical homogeneity, requires low processing temperatures, and gives the ability to precisely control particle size and morphology [47].

Solvent casting: A solvent is used to dissolve a selected polymer. In this solution, a porogen, a water-soluble salt compound, is added, and the final solution is cast in a preferred mold. The solvent used is then allowed to evaporate, leaving behind the polymer with the salt compound. This is followed by a particulate leaching step, whereby the salt is leached with water, effectively resulting in a porous scaffold. By regulating the amount and size of the porogen used, the outcome can be tailored to achieve a desired porosity and interconnectivity [48].

Freeze gelation: a polymer solution is frozen beforehand and the solidified sample is then immersed in a non-solvent maintained at a temperature below the freezing point of the polymer solvent. While in this state, crosslinking agents in the non-solvent initiate the gelation of the polymer. During this process, the non-solvent slowly replaces the ice crystals formed from the polymer solvent. This controlled exchange leads to the formation of a porous hydrogel structure, as the ice sublimates and is substituted by the non-solvent phase [49].

Electrospinning: A jet of a liquid polymer is spun onto a plate using a high voltage under ambient conditions. Nonwoven fibers are generated when the applied electric

voltage exceeds the polymer droplet's surface tension, inducing electrostatic forces that elongate the liquid into fine filaments [12]. They are then deposited onto a collector with an opposite charge. Electrospinning parameters such as polymer concentration, voltage, and flow rate significantly influence fiber morphology. It enables the fabrication of nanofibrous structures with high surface area, making them suitable for biomedical and tissue engineering applications.

3D printing: A rapidly growing method under additive manufacturing. It has presented a great opportunity in BTE. Compared to the above methods, this field ranks superior when it comes to design control, reproducibility of multiscale 3D tissue structures, and other parameters. It generally refers to the layer-by-layer construction of the scaffolds. There are several different techniques in this additive manufacturing field including, vat photopolymerization, powder bed fusion, and 3D bioprinting.

3.4. Structural concepts of BTR scaffolds

Scaffolds required for BTR relate to the retrofitting elements used in construction, treating cracks or fractures. A proper geometrical design and structural analysis would ensure an efficient, regeneration-oriented output. The following sections explain the different design and analysis methodologies applied in this field.

Geometric design

Scaffold architectures in BTE are broadly classified into non-parametric and parametric categories [50]. Non-parametric scaffolds are constructed using simple periodic geometries such as simple cubic, body-centered cubic (BCC), face-centered cubic (FCC), octet truss, truncated octahedron, and diamond configurations. However, this lattice-based scaffolds face limitations in simultaneously achieving high porosity and mechanical strength [51]. In contrast, parametric scaffolds are designed through mathematical modeling and algorithm-driven strategies to produce complex and customizable scaffold geometries. The main examples are Triply Periodic Minimal Surfaces (TPMS) and Voronoi-based structures.

TPMS-based scaffolds: Scaffolds based on TPMS are mathematically designed structures that exhibit continuous, repeating geometries with highly ordered porosity [52]. The repeating geometries are based on unit cells that could assume different shapes as shown in Fig. 3.5 below. Their interconnected porous and curved architecture mimics that of trabeculae bone is beneficial for cell attachment, proliferation, and bone tissue regeneration [53].

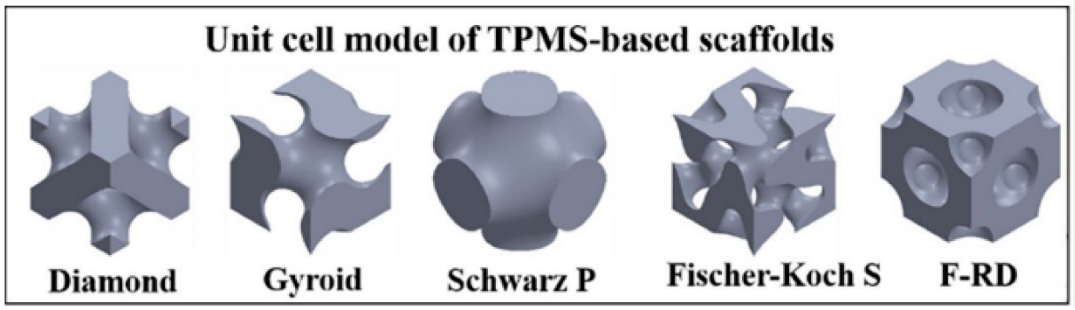

Figure 3.5: Fundamental TPMS unit cell basis [54]

Voronoi-based scaffolds: These, on the other hand, are generated through Voronoi tessellation, a computational geometrical design based on the Voronoi pattern. It has high resemblance to several patterns in nature, including the trabecular bone. In this method, as shown in Fig. 3.6, a certain region is populated with randomly distributed seed points that define polyhedral cells scaled to create pore networks and struts.

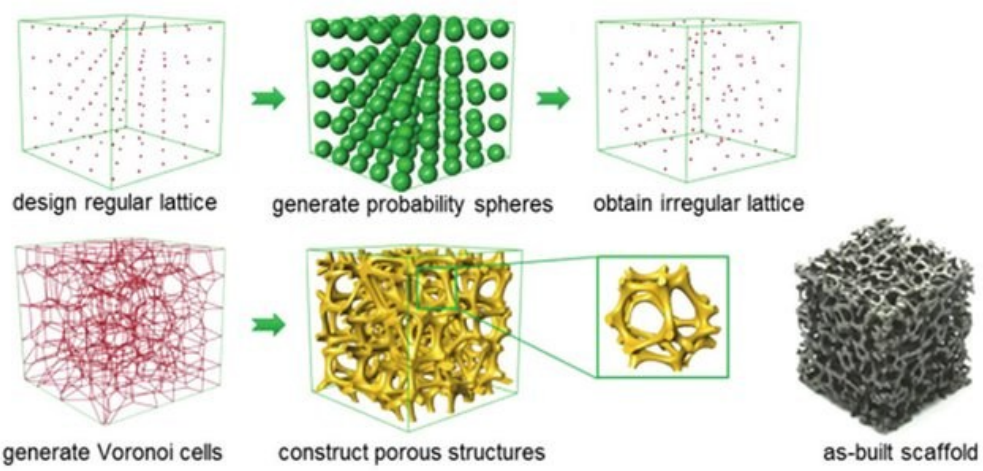

Figure 3.6: Diagram showing the scaffold design principle based on the Voronoi-Tessellation method [55]

This stochastic design approach allows for structural heterogeneity, which better replicates the anisotropic mechanical behavior of native bone while maintaining sufficient porosity for vascularization and osteointegration [50].

Finite element analysis

In BTR scaffolds, finite element analysis (FEA) is a numerical tool of analysis that uses partial differential equations to solve stress functions after discretizing the scaffold into a finite number of elements [56]. Components such as displacement,

principal strain, component strain, principal stress, and von Mises stress are calculated [50]. An algorithm of how FEA is conducted is shown in Fig. 3.7 below. FEA is a vital tool in BTE as it gives information on how the scaffold behaves upon implantation and contributes to the optimization of the design with less trial and error.

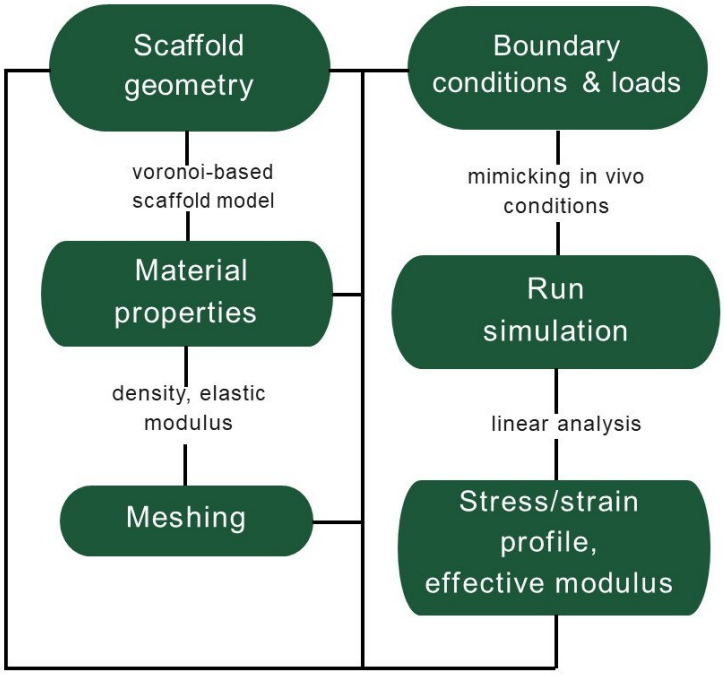

Figure 3.7: Algorithm for FEA analysis of BTE scaffolds

Computational fluid dynamics

Computational fluid dynamics (CFD) is used to investigate the microfluidic environment that tissue scaffolds are subjected to. It also helps understand the effect of nutrient transport on the growth of cells and how this growth is maintained as tissues regenerate at the expense of the implanted scaffolds [57]. The resulting fluid flow between the scaffold and tissues induces a wall shear stress (WSS) on the cells. WSS plays a critical role in regulating the biological responses of mesenchymal stromal cells. A range of 0–30 MPa enhances the overall cellular activity, including proliferation and metabolic function, 0.11–10 MPa can promote osteogenic differentiation, and high stress of 0.55-24 MPa stimulates matrix mineralization in bone-forming cells [58].

4. AIM OF DOCTORAL STUDY

This doctoral thesis is entitled "Bio-based scaffolds for Bone Tissue Regeneration". It combines the disciplines of material science, engineering, chemistry, and biomedical sciences. It mainly deals with the fabrication of a biocompatible and reproducible tissue scaffold with enhanced properties for bone tissue regeneration. Moreover, sustainability is at the core of its contribution to the field. The major objectives of this work can be summarized as follows.

- **Assess environmentally friendly biomaterials and synthesize from sustainable sources**. The biomaterials selected for scaffold fabrication are bacterial cellulose, graphene oxide, hydroxyapatite, and cellulose acetate. This study ventures into the sustainable sourcing of biomaterials by synthesizing the first three from renewable, abundant biomass and food waste. (Publication I, Publication II)
- **Design, produce, and characterize efficient scaffolds for BTR**. Since the main purpose of this study is to develop functional scaffolds, the design and subsequent evaluation of the prepared scaffolds is one of the core deliverables. Various characterization techniques as well as testing procedures will be performed, highlighting the necessary data obtained. (Publication II, Publication III)
- **Evaluate the biocompatibility of prepared scaffolds using both cell-based (in vitro) and animal model (in vivo) studies.** The integration of the scaffolds with cells is the basis of their ability to serve as platforms. This calls for the cytocompatibility of each scaffold and its capacity to promote cell adhesion and proliferation once implanted. Thus, this study performs evaluations of the scaffolds for the above requirements both in vitro and in vivo. (Publication IV)
- **Perform functional analysis for final optimized scaffold design for the purpose of bone tissue regeneration.** The structural viability of a scaffold when it comes to absorbing and dissipating the stresses that it is subjected to is vital to determine its final output. The stresses could be generated from internal loads or fluidic environments surrounding bones. Hence, this study looks into the computational analysis of a scaffold using finite element analysis. (Publication V)

5. EXPERIMENTAL SECTION

This chapter outlines the key components of the study, including the biomaterials to be used, scaffold fabrication techniques, characterization methodologies, and computational analyses. It provides detailed procedures for each aspect, with particular emphasis on critical steps and considerations.

5.1. Biomaterial synthesis

Bacterial cellulose

BC was synthesized using *Komagataeibacter xylinus* bacterial strain in a Hestrin−Schramm (HS) growth medium supplemented with an equal amount of apple juice. The HS medium consisted of 20 g glucose, 5 g yeast extract, 5 g peptone, 2.7 g disodium hydrogen phosphate, and 1.15 g citric acid in 1 L total volume of deionized (DI) water. Whereas the juice was prepared from waste apples sourced locally. 5 ml of HS medium was first used to activate 5 loops of the bacterial strain. After 3 days of incubation, this was added to 100 ml of previously prepared HS/apple juice medium. BC pellicles were then harvested from this culture after 2 weeks of static incubation at 30 ºC.

For purification purposes, the produced BC pellicles were washed with DI water, followed by boiling in a 0.5 N NaOH solution at 80 ºC for 1 h. The pellicles were again washed with DI water repeatedly until a neutral pH was maintained. The BC mats were then either kept at 4 ºC for further processing or freeze-dried for immediate experiments.

Graphene oxide

GO was prepared from another household food waste – spent coffee grounds. The biomass was first thoroughly washed to remove any unwanted material and soaked in an iron salt ($FeCl_3.6H_2O$) for 24 h for catalytic graphitization at a lower temperature [59]. The sample with the iron catalyst was dried overnight and then graphitized in a tube furnace at 1000 ºC for 2 h under Ar gas flow. Thereafter, to remove the iron salt and get the graphitized carbon material, it was soaked in concentrated HNO_3, followed by washing with DI water. To obtain GO, the standard modified Hummer's method was used [60]. The obtained product was ultrasonicated to obtain well-dispersed GO particles.

Hydroxyapatite

Hydroxyapatite (HAp) was synthesized from eggshells, obtained from a personal kitchen, as a natural source for calcium and H_3PO_4 as the phosphorus source. The eggshells were washed, oven-dried for 12 h, and manually ground to obtain particles. The resulting powder was subjected to thermal decomposition in a tube furnace at 1000 ºC for 2 h to acquire CaO. Thereafter, the CaO was mixed with DI water to form a 0.5 M $Ca(OH)_2$ solution. A 0.3 M H_3PO_4 acid solution was then introduced to the solution dropwise at a controlled rate of 2 ml/min to maintain the desired Ca/P molar ratio. This mixture was aged for 48 h to facilitate complete reaction and phase development. The precipitate, filtered, was thoroughly washed with DI water to eliminate residual ions and oven-dried overnight. As a last step, it was further calcined at 700 ºC for 2 h in a tube furnace to promote crystallization and obtain the final HAp powder.

5.2. Scaffold fabrication

Using the above biomaterials as building blocks, scaffolds will be fabricated. Three different methods will be used to obtain varying typologies. This section discusses the methodologies to be used.

In situ hydrogel synthesis

Hydrogel scaffolds were prepared using BC mat as a base material. GO and HAp, prepared in the methods explained in the previous section, were used as filler/reinforcement materials. The process involved adding 1 mg/ml of GO (in DI water) and 2 mg/ml of HAp (in DI water) during the synthesis of BC. The mat was left to form for an additional 7 days in the modified medium. At the end of the 15th day, the reinforced pellicles were removed and purified in the same process as that of the pure BC mat.

Electrospinning

In this section, a polymeric composite consisting of cellulose acetate (CA) (average Mn ≈ 50,000) and GO was used for electrospinning. GO solution was prepared in a 1:1 vol ratio of DMAc: acetone solvent mixture at a concentration of 5 wt% of the polymer (CA) and ultrasonicated. Afterward, CA (15 wt% of the total solution) was added. Electrospinning was then performed in an EC–DIG apparatus (IME Technologies, Waalre, The Netherlands). The electrospinning parameters for optimal CA fibers (25 ºC and 65–70% humidity) were used. A flow rate of 0.1 ml/h

and a high voltage of 13 kV were maintained to create the polymer filaments from the nozzle kept 20 cm away from the collecting drum.

5.3. Characterizations and testing

Morphology

The structure and morphology of particles need to be studied as it affects the intended outputs. For this purpose, samples were analyzed using scanning electron microscopy (SEM) (FEI, Brno, Czech Republic). To capture and identify specific elements present in the compositions, energy-dispersive X-ray (EDX) spectroscopy was utilized as fit. Prior to microscopy, the samples were dried and attached to double-sided carbon tape and sputter-coated with Au−Pd particles.

Crystallinity

It is essential to understand the crystalline phase and intensity of the materials used. Hence, to identify this and the subsequent diffraction patterns, an X-ray diffractometer (XRD) (MiniFlex 600, Rigaku, USA) was utilized. The measurements were taken using a Co target with Kα radiation (wavelength of 1.79 Å) operated at 40 kV and 15 mA. 2θ values were read between 4º and 80º. For the convenience of reporting, the intensities gained were then converted to Cu-Kα radiation using a PowDLL converter, version 2.911.0.0.

Functional groups

Since the molecular composition affects the formation of bonds in a composite, the functional groups in the biomaterials need to be studied. These groups in the biomaterials and scaffolds were identified using Fourier transform infrared (FTIR) spectroscopy in attenuated-total reflectance mode (Nicolet Is5, Thermo Scientific, USA). The scanning frequency range was 4000−400 cm^{-1}.

Mechanical testing

Tensile strength of the fabricated scaffolds was measured using a universal testing machine (Model M350-5CT, Testometric, UK). Rectangular test specimens were prepared with dimensions of 10 × 40 mm, and a gauge length of 20 mm was maintained between the test grips. The thickness of each strip was measured using a digital thickness gauge (Mitutoyo, Germany) prior to testing. A constant crosshead speed of 10 mm/min was applied under a 1 kg load cell. Tensile stress and strain

values were then recorded up to the point of failure. The apparent Young's modulus was calculated from the slope of the linear elastic region of the stress–strain curve. All measurements were performed in n = 5 for each sample group to ensure statistical reliability.

Thermal degradation

The thermal stability/degradation of the samples was assessed by thermogravimetric analysis (TGA) using a TGA Q500 device (TA Instruments, USA). The tests took place under a nitrogen atmosphere (60 $ml.min^{-1}$) in a temperature range of 25−800 ºC and at a heating rate of 10 ºC/min.

5.4. Biocompatibility studies

Given that biocompatibility and the absence of cytotoxicity are critical determinants of a scaffold's suitability for clinical application, comprehensive evaluations were performed. The following sections detail the methodologies employed for both in vitro and in vivo assessments of the fabricated scaffolds.

In vitro model

In the indirect testing, 10 µl of FBS was added at 30–32 ºC to adhere the sterilized samples to each well surface. Afterward, culture medium containing 90% DMEM and 10% FBS enriched with antibiotics (100 U/mL penicillin and 100 g/mL streptomycin) was added to the wells. The same was done to control wells not containing samples. The setup was then incubated in a humidified atmosphere at 37 ºC with 5% CO_2 in air for 1, 3, and 5 days. The cell culture medium (including sample extracts and control medium) was harvested and used in the following experiment. For the cell viability study, human osteosarcoma Saos-2 cells were plated in 96-well flat-bottomed microplates at a concentration of 1.0×10^5 cells/well in fresh DMEM medium supplemented with 10% FBS and antibiotics. After 24 h, the culture medium was removed from each well and replaced with 100 µl of DMEM in the wells that contained extracts obtained after 1, 3 and 5 days of incubation periods and the control. Then, the standard MTT assay protocol was conducted in the following procedure. After 72 h, MTT (3-(4,5-dimethylthiazol-2-yl)-2,5-diphenyltetrazolium bromide) colorimetric test was utilized to investigate the viability of cells under the influence of the scaffolds. The process was as follows. The Saos-2 cells were incubated in MTT solution (0.5 mg/ml in DMEM) at 37 ºC in a CO_2 incubator (5% CO_2 and 95% air) for 3 h. Afterward, 1:1 (vol/vol) ratio of absolute ethanol and DMSO was used to dissolve the blue formazan. The microplate was shaken briefly,

and measurements were taken by an ELISA automatic microplate reader (TECAN, Sunrise™, Grodig/Salzburg, Austria) at a wavelength of 540/620 nm optical density. Relative cell viability was expressed as a percentage relative to the control group (taken as 100% viability).

In vivo model

Animal studies were conducted in association with the Institute of Experimental Morphology, Pathology, and Anthropology under the Bulgarian Academy of Sciences. 18 female BALB/c mice (4–5 months old) were obtained from a licensed laboratory animal breeder, and experiments were conducted in compliance with national regulation No. 20/01.11.2012 on laboratory animals and animal welfare, as well as the European Directive 2010/63/EU. The experiment involved surgical implantation of scaffolds in five groups of mice (3 per group), and each group was assigned to a specific scaffold as stated in Table 5.1 below. In groups G1-4, implants were designated to the back-right leg, whereas in group G5, the scaffolds were designated to the parietal bone (part of the calvaria). A control group was void of any surgical intervention.

Table 5.1: Implant scaffolds' biomaterial composition for the five groups of mice

Materials	**G1**	**G2**	**G3**	**G4**	**G5**
BC	mat	mat	mat	mat	mat
HAp	-	2 mg/ml	-	2 mg/ml	2 mg/ml
GO	-	-	1 mg/ml	1 mg/ml	1 mg/ml

Surgical procedure

Prior to surgery, anesthesia (a combination of ketamine (25 mg/ml) and xylazine (1.2 mg/ml)) was administered. In G1-4, the skin was carefully lifted from the underlying muscle, and 5 mm diameter implants were placed deep within the popliteal fossa. In G5, following superficial abrasion of the external surface near the parietal eminence, 5 mm diameter implants were inserted and covered with muscle tissue. They were all then disinfected with ethanol (70%) and Braunol (7.5% w/w) iodinated Povidone cutaneous solution. Finally, sterile sutures were put in place, and a single dose of Baytril was administered. Following surgery, monitoring was performed three times per day during the first week, then reduced to once daily, with no requirement for topical therapy. After 60 days, the mice were sedated with ketamine/xylazine before euthanasia, followed by blood collection for analysis.

Histopathological examination

Tissue specimens were harvested from the surgical site for histological evaluation. Samples were fixed in 10% neutral-buffered formalin, followed by a standard protocol involving dehydration, cleaning with xylene, and embedding in paraffin. Sections of 3–5 μm thickness were prepared and stained with hematoxylin and eosin (H&E). Histological analyses were performed using a Leica DM 5000B light microscope (Wetzlar, Germany).

5.5. Computational analysis

Design and analysis of a theoretical scaffold is shown in this part of the experiment to investigate the structural viability of Voronoi-based scaffolds to be used for BTR.

Voronoi-based scaffold design

A 3D scaffold model of 12 × 12 × 12 mm was generated using the Voronoi tessellation technique to replicate the irregular porous architecture of trabecular bone. The design process was carried out using the software suite Rhinoceros 3D (Version 8) with the Grasshopper plug-in. Within the defined cubic design space, a randomized distribution of seed points was generated to serve as the basis for Voronoi cell formation. These seed points determined the spatial arrangement and connectivity of the struts, resulting in an interconnected porous network suitable for tissue ingrowth and vascularization.

Finite element analysis

The Voronoi model was imported to ANSYS 2025 R1 (ANSYS Inc., Canonsburg, PA, USA). The scaffold models were meshed via ANSYS Meshing. PLA was assigned as a scaffold material. Boundary conditions were defined by constraining the bottom surface in all degrees of freedom, while a uniform load of 1.5 MPa was applied on the top surface of the scaffold by attaching a rigid plate. A finite element method (FEM) analysis was then conducted to evaluate the scaffold's mechanical response, including von Mises stress distribution and displacement.

6. RESULTS

This section discusses the obtained results as summaries from the publications achieved as part of the work. It highlights the publications' findings in terms of material outputs, characteristics, and their potential applications. It also enumerates the results of the computational analysis of the performance of a theoretical scaffold subjected to loading conditions resembling those in the human body.

6.1. Synthesized biomaterials

On average, 5 mm-thick BC pellicles were harvested after 14 days of incubation (Fig. 6.1a & b). Morphological analysis of BC was done using SEM, and the image in Fig. 6.1c revealed an interconnected nanofibrous structure **(Publication III).** It also possesses sufficient porosity, which is a sought-after property as a scaffold. Individual fibers were measured to have an average diameter of 80±2 nm. This nanoscale size increases the surface area of the fibers, which in turn gives the high water retention capacity of BC [61].

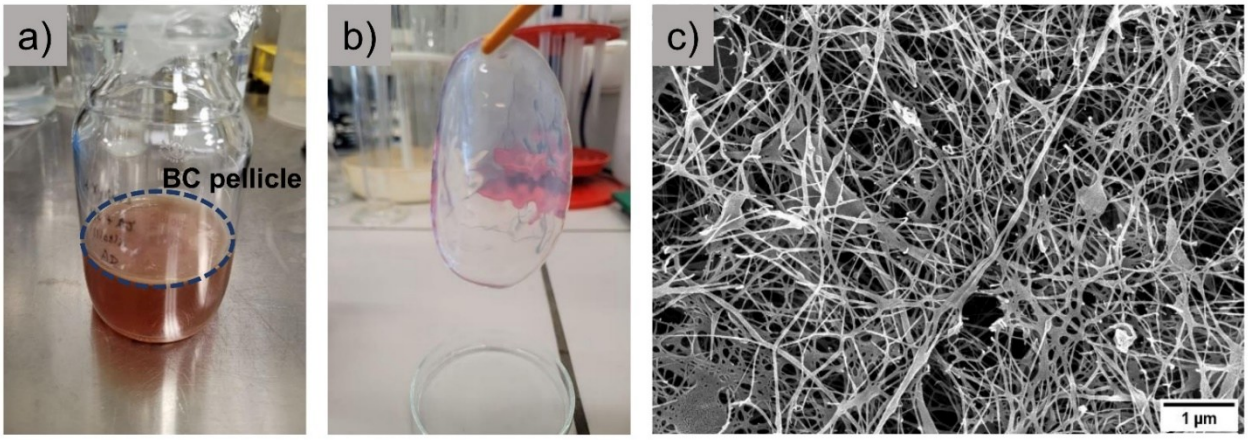

Figure 6.1: Synthesis of BC using waste apple juice & HS medium (a), purified BC mat (b), and SEM micrograph image of BC nanofibers (c)

FTIR spectra showed the composition of the functional groups found in BC as shown in Fig. 6.2a below. A broad peak at 3347 cm^{-1} showed the characteristic -OH stretching vibration, whereas a peak at 2893 cm^{-1} can be attributed to the aliphatic C-H stretching vibration [62]. In addition, the spectra also showed an asymmetric C−O−C stretching vibration at 1110 cm^{-1} and a C−O stretching frequency of the cellulose glycosidic links at 1056 cm^{-1} [63]. On the other hand, XRD results showed the characteristic diffraction profile of cellulose I_{β}, in Fig. 6.2b.

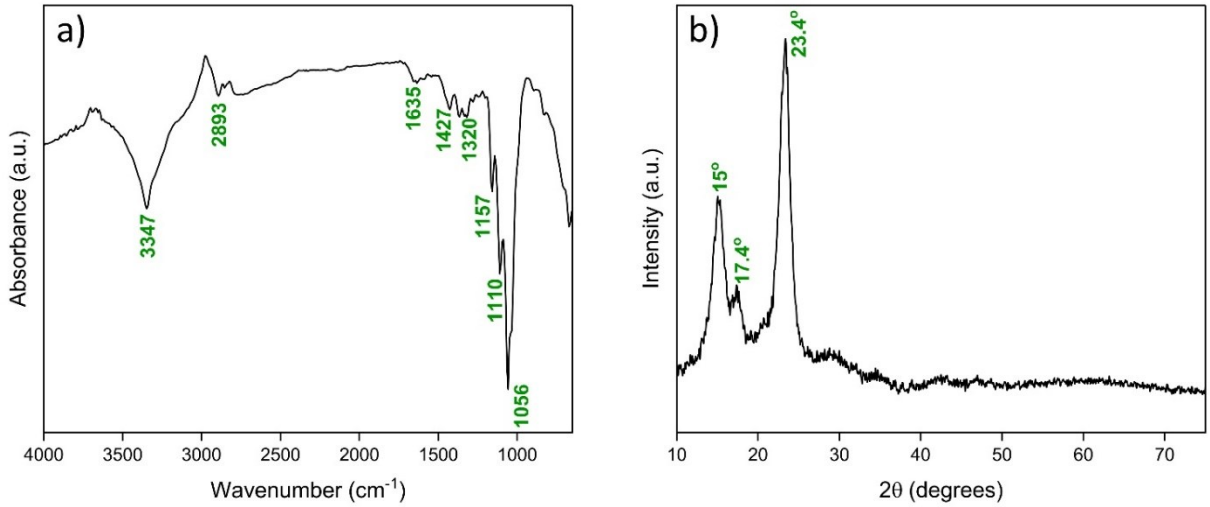

Figure 6.2: Characteristics of produced synthesized BC depicted by FTIR spectra (a) and XRD spectra (b) graphs [64]

In order to investigate the quality of its molecular arrangement, the crystallinity index of BC was calculated using the following equation.

$$\mathrm{CI}\ (\%) = \frac{\text{Area of crysslltine peaks}}{\text{Total area of peaks}} * 100; \tag{6.1}$$

Where the peaks are taken from the values of the XRD graph (Fig. 6.2b).

This gave a result of 77.4 % which confirms the high crystallinity yield that characterizes *Komagataeibacter xylinus* in contrast with other bacterial strains, which range from 60-80% [63, 65]. This contributes to its mechanical strength and controlled degradation, both required properties in tissue regeneration [61].

GO was produced from spent coffee grounds. There are various organic sources for of GO, including coconut shells, sugarcane bagasse, rice straw, sawdust, tea leaves, and others [66]. This study chose spent coffee grounds as the source for GO. They are abundant and relatively easier to process into graphite (GO precursor) since their carbon content is high **(Publication I).** Coffee waste contains 51% carbon and 38% oxygen, among other trace minerals [67]. To avoid the high pyrolysis temperature needed to graphitize the precursor, an iron chloride salt was used as a graphitization catalyst, as discussed in **Publication III.** The SEM image in Fig. 6.3a shows layers of GO flakes. Fig. 6.3b shows the XRD peaks of the produced GO, whereby an amorphous structure is depicted. This is different from the expected sharp peak at 11° of GO produced from actual graphite. The structural differences in

morphology and crystallinity between the synthesized GO and the commercial one arise because it is sourced from a biomass precursor [68].

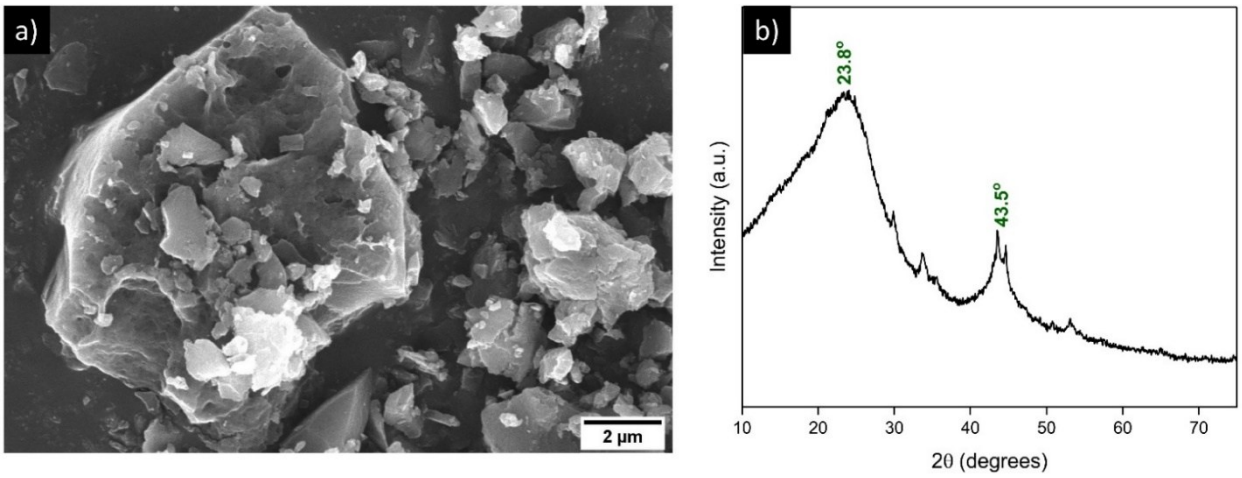

Figure 6.3: SEM image of individual and agglomerated GO flakes (a) and the corresponding XRD spectra [64]

HAp was synthesized using eggshells as the primary calcium source. The characteristic nanorod-shaped nanoparticles are shown in Fig. 6.4a, agglomerated after the second heat treatment. Based on the EDX spectra presented in Fig. 6.4b, the Ca/P ratio of the synthesized HAp was calculated to be 1.72, which is reasonably close to the theoretical value, 1.67 **(Publication III)**. The slight increase in the Ca/P ratio observed in the synthesized sample can be attributed to the probable unreacted, residual calcium oxide (CaO), resulting after the combined calcination process [69].

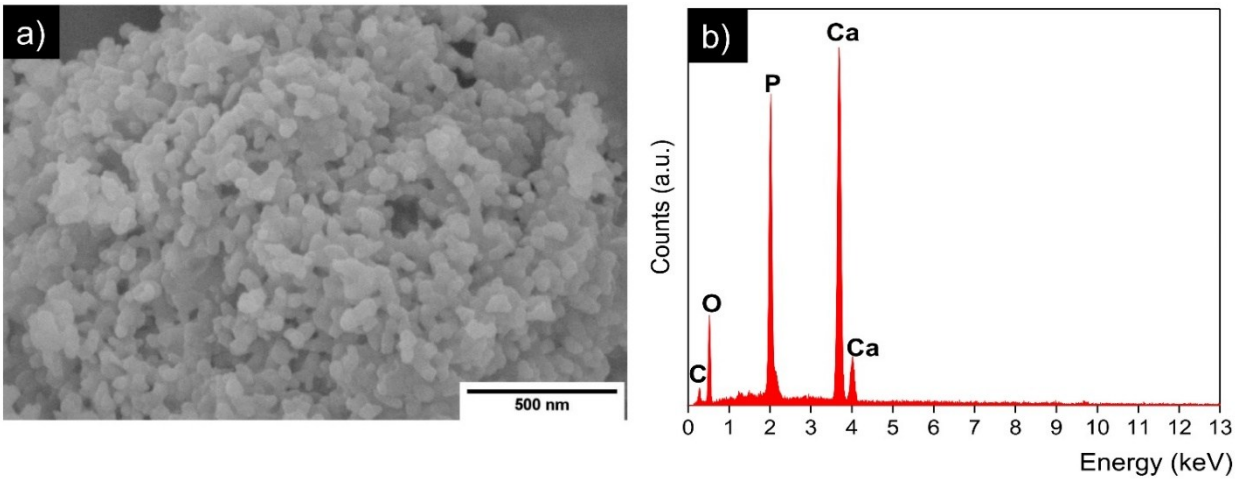

Figure 6.4: SEM image of HAp nanoparticles produced from egg shells (a) and the corresponding EDX spectra (b) [64]

6.2. Fabrication of scaffolds

As explained previously, among the various techniques of producing scaffolds for BTR, two methods are used in this study. They were chosen for simplicity, efficiency, and desired yield. In the following subsections, the processes and the key results are summarized.

Electrospinning

CA is a biopolymer that can be efficiently electrospun into a scaffold, as described thoroughly in **Publication II** of this thesis. An average of 458 ± 158 nm fiber diameter was measured. which was well embedded into the CA fibers as seen in Fig. 6.5a below. The incorporation of GO particles led to minimal bead formation along the fibers and resulted in a lower water contact angle compared to that of pristine CA fibers, indicating improved surface wettability. More importantly, the addition reinforced the mechanical properties of the scaffold, as evidenced by the tensile strength comparison between pure CA and the biocomposite scaffold shown in Fig. 6.5b. This improvement is primarily attributed to the formation of intermolecular hydrogen bonds between CA and the hydrogen-containing functional groups present on the GO particles.

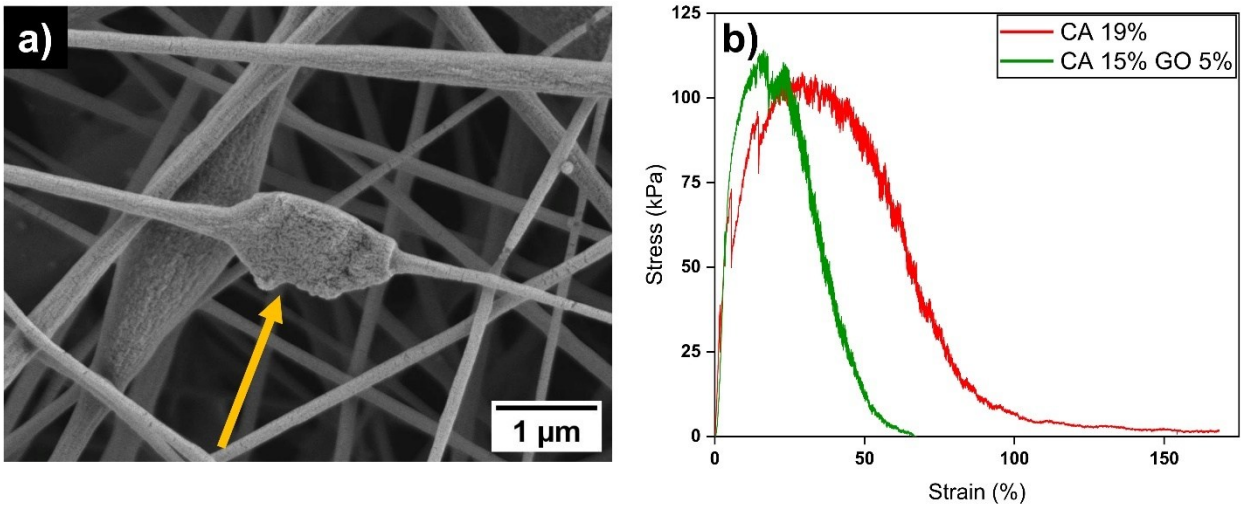

Figure 6.5: SEM image of CA nanofibers with embedded GO nanoparticles indicated by the arrow (a), tensile stress-strain curve for electrospun scaffolds with pristine CA and CA/GO scaffolds (b) [60]

In addition, it was observed that the addition of GO did not pose cytotoxicity to the biocompatible nature of CA, in an in vitro study performed using osteoblast-like MG-63 cells. The scaffolds containing GO exhibited a cell viability value of more

than 70% (compared to the control group), and the cells appeared to adhere and spread onto the surface of the scaffold. This indicates that the oxygen-rich, hydrophilic, and flexible structure of GO promotes cell growth and expansion [70].

In situ biosynthesis of hydrogel

BC mat possesses valuable characteristics of a hydrogel scaffold. This is due to its fibrous structure at its core. The incorporation of the reinforcements (GO and HAp) into the growing BC pellicle was intended to enhance its mechanical and biocompatible nature. The results showed a biocomposite with incorporated particles as discussed thoroughly in Publication III.

A highlight of this study was the improvement of the mechanical property of the composite through the addition of GO, as shown in Fig. 6.6a below. The BC/GO and BC/HAp/GO sheets demonstrated a 24.73% and 18.74% increase in tensile strength, respectively, compared to pure BC strips. This was due to the strong hydrogen bond formation between the components mainly through the functional groups of GO [71]. Whereas, HAp significantly improved the thermal stability of the composite scaffold as shown in the TGA result in Fig. 6.6b. This was possibly due to the physical cross-linking within the composite, which increased the functionalization of the BC matrix [72].

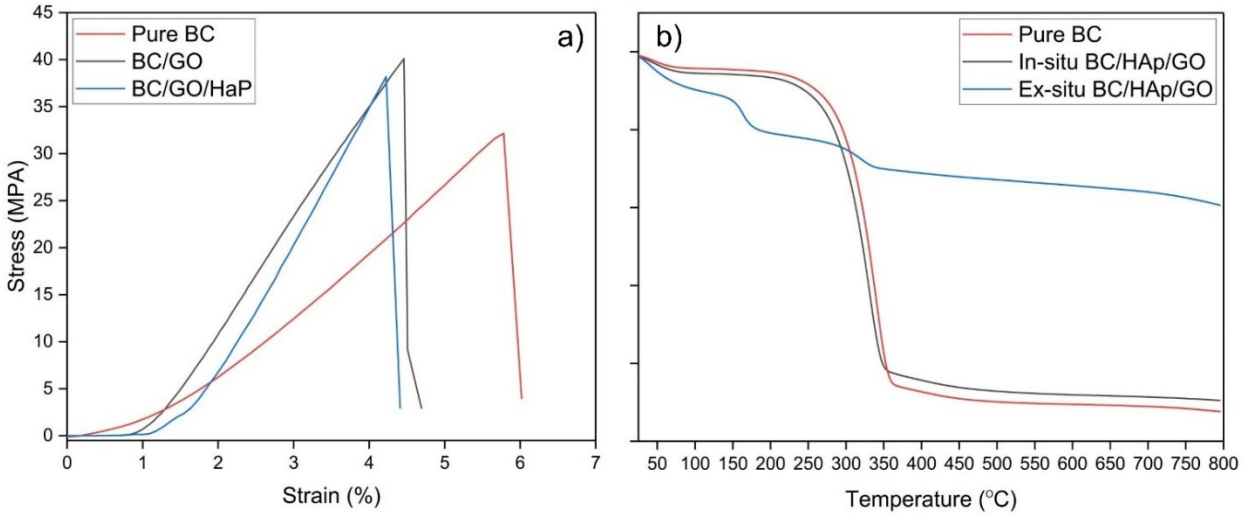

Figure 6.6: Tensile stress–strain graph (a) and TGA results (b)of pure BC and its composites [64]

6.3. Biocompatibility assessment

As biocompatibility of BTR scaffolds is a deciding factor for their potential use, in vitro and in vivo studies were made and thoroughly discussed in Publication IV (submitted) of this thesis. In vitro studies were performed using human osteosarcoma Saos-2 cells, and an in vivo procedure was performed on Balb/c mice. Fig. 6.7 below shows the results for cell viability of pure BC and composite scaffolds including GO, HAp, and both. It was found that all scaffolds showed required viability (>70%). Those that incorporated HAp particles resulted in the highest, showing that cells were able to spread and proliferate better than the control and the pure BC scaffolds. This proves the positive influence of HAp on the osteogenic performance of scaffolds, given its surface properties and calcium/phosphate composition [73].

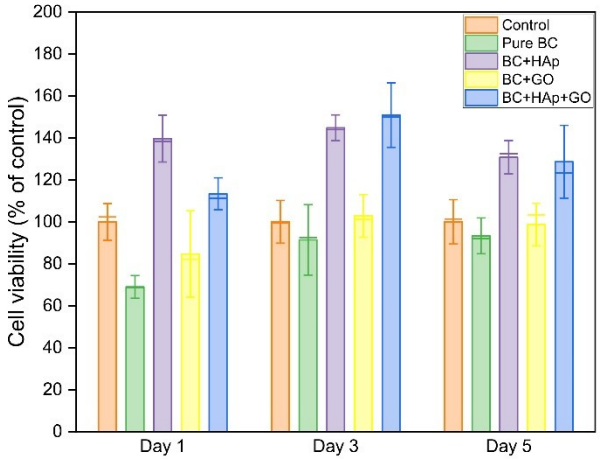

Figure 6.7: In vitro cell viability study results using Saos-2 cells

The regenerative capability of the scaffolds has been well identified through the histological analysis that was carried out. Pure BC scaffolds resulted in the formation of large granulation tissues as shown in Fig. 6.8a. Whereas, in Fig. 6.8b, the integration of the implant with the host tissues, subsequent osteoblast growth is evident. This highlights the osteoconductive properties of HAp [74]. In Fig. 6.8c and d, a higher number of capillaries were seen, ascertaining the role that GO plays in angiogenesis and general bone healing processes [75].

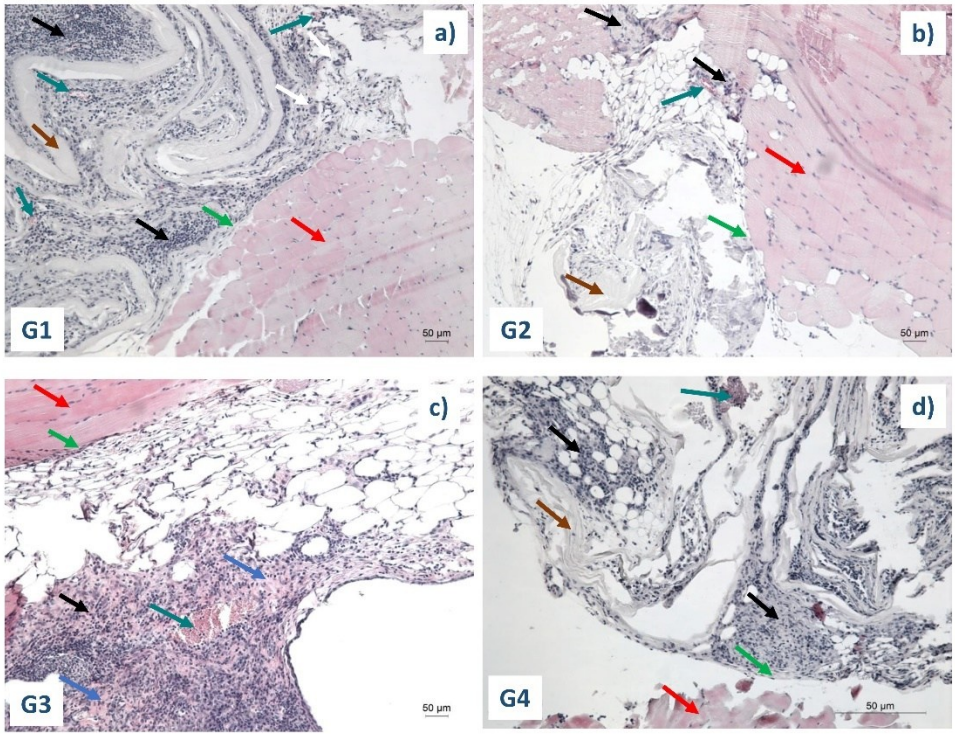

Figure 6.8: Representative images of histological results using HE staining. The implants were situated in the fossa poplitea (a-d) (scale bar: 50 µm). Arrows indicate the following; Black arrows - granulation tissues, red arrows - muscle tissues, green arrows - very thin fibrous capsule, brown arrows - the implant fibers, blue arrows - fibrin and collagen fibers in granulation tissue, Yellow arrows – bone matrix with osteocytes, Teal arrows– capillaries, white arrows- giant cell of foreign body type

6.4. Structural concepts

Voronoi-based scaffolds are generated through Voronoi tessellation, a computational geometry method in which a predefined set of seed points divides a volume into irregular, cell-like partitions. This architecture closely mimics the morphology of trabecular bone, providing an interconnected porous network that can significantly support cell attachment, migration, proliferation, and ultimately tissue regeneration.

Here, a 12x12x12 mm^3 scaffold, with average an strut diameter of 0.8 mm and a pore size of 2 mm, was modelled, as illustrated in Fig. 6.9 below. As can be seen, the irregular arrangement of the struts highly resembles the natural architecture of the spongy part of the bone, with varying sizes of pore spaces, which play an essential role in the differing requirements needed for cell growth and the transportation of nutrients.

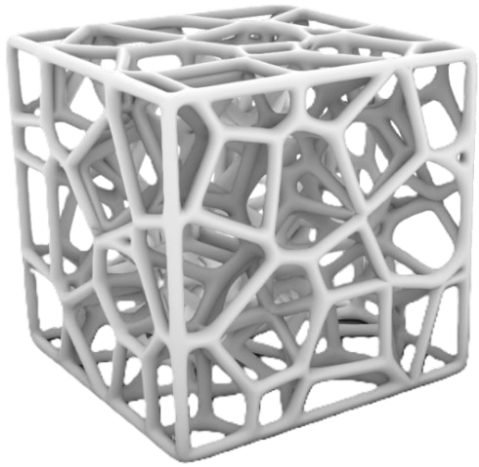

Figure 6.9: Design of Voronoi-based scaffold

Finite element analysis

FEA Finite Element Analysis (FEA) is a computational technique used to predict the structural response of a material or object by discretizing its geometry into a mesh of smaller, finite elements. In this study, FEA was employed to simulate the mechanical behavior of a scaffold under physiological loading conditions, mimicking its performance at a potential surgical implant site. The analysis focused on the Voronoi-based scaffold model introduced above. The analyses and output of this section is scheduled to be included in **Publication V** of this thesis.

To optimize computational efficiency, a representative volume element (RVE) ($2.5 \times 2.5 \times 1.75$ mm^3) was extracted from the full scaffold geometry. It was selected to include at least one interconnected pore and a sufficient number of struts, ensuring it accurately reflected the scaffold's local structural features. PLA was assigned as a scaffold material because it is regularly used for 3D printing of BTR scaffolds. A surface load of 1.5 MPa was applied to account for a full body weight and increased loads due to exercises and movement.

The major results are depicted in Fig. 6.10 below. The maximum total deformation was 94.2 μm at the top of the scaffold with open branches (as a result of the cut). This can be taken as minimal. This value can be minimized by reducing the size of the pores and manipulating their configurations [76]. The maximum von-Mises equivalent stress was found to be 263.5 MPa. This value was recorded at the connection point of the struts, which is the weakest link [77]. In addition, it is higher than the compressive strength of PLA (60 MPa) [76]. Hence, it necessitates an incorporation of reinforcements such as GO that has been extensively discussed in this study.

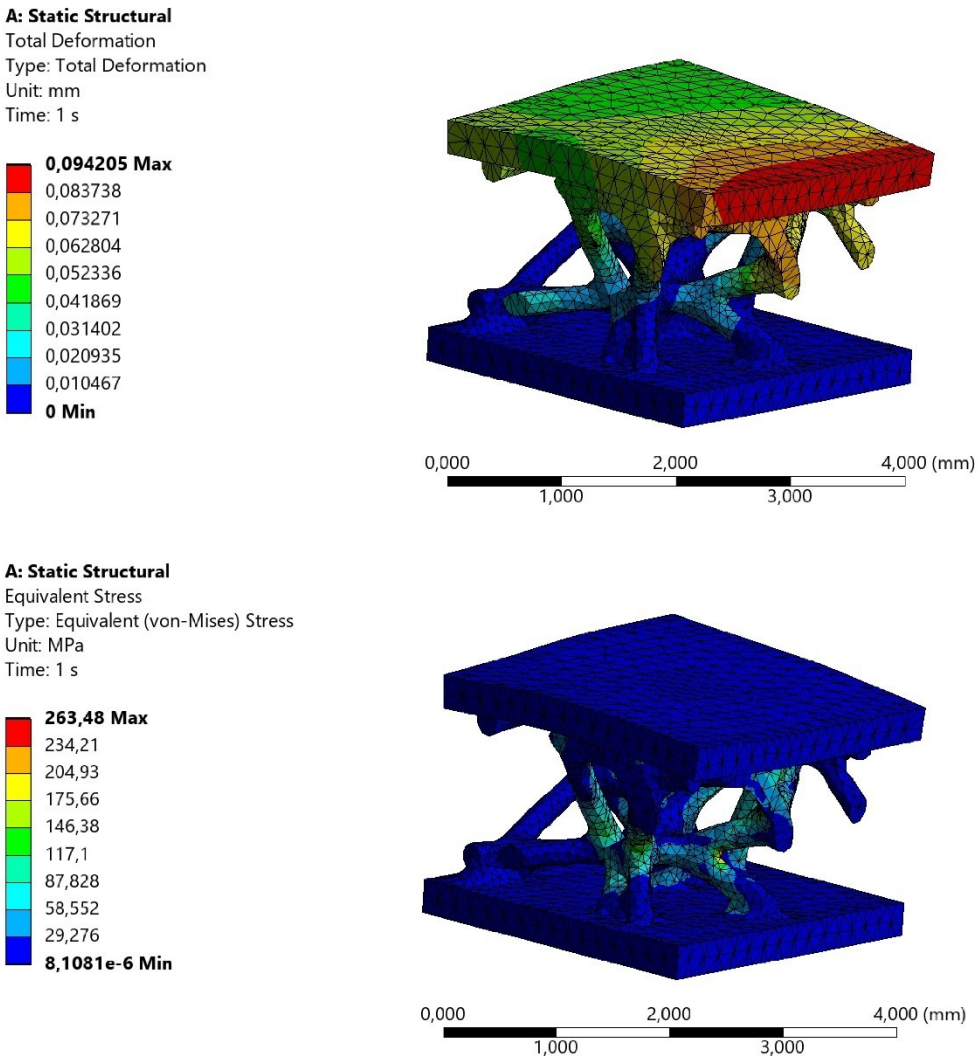

Figure 6.10: FEA results for RVE model describing the total deformation and equivalent stress

7. CONCLUSION AND CONTRIBUTION OF THE WORK

This thesis explored the advancing field of BTE and focused on the development of sustainable, better-performing scaffolds for the purpose of BTR. These biocomposites were synthesized from sustainable sources and through various characterizations techniques, it is identified that the resulted BC, GO and HAp either resemble or behave exactly as their commercial counterparts. The methods used to fabricate the biocomposite scaffolds also resulted in desired attributes. The biocompatibility study was vital in ensuring the potential application of the materials for actual medical use. Scaffolds with HAp nanoparticles showed the highest cell viability, followed by those containing HAp and GO. This outlines the osteogenic potential of the biomaterials used. In vivo studies of the scaffolds using laboratory mice also showed promising results. Histology results from in vivo studies also showed indicated growth of granulation tissues, absorption of scaffolds into host tissues, and ample neovascularization.

This research would contribute to the growing body of work promoting green synthesis approaches in biomedical engineering and offers potential alternatives for the development of efficient scaffold systems for regenerative medicine. Such approaches are particularly relevant in today's world, where a growing global population faces challenges related to chronic illness, trauma, and limited access to effective treatment. By emphasizing cost-effective, scalable, and high-performance solutions, this work supports the vision of a more inclusive and accessible future in healthcare.

REFERENCES

1. Olson, J.L., A. Atala, and J.J. Yoo, *Tissue engineering: current strategies and future directions.* Chonnam Med J, 2011. **47**(1): p. 1-13.
2. Oftadeh, R., et al., *Biomechanics and mechanobiology of trabecular bone: a review.* J Biomech Eng, 2015. **137**(1): p. 0108021-01080215.
3. Lindsay M. Biga, S.B., Sierra Dawson, Amy Harwell, Robin Hopkins, Joel Kaufmann, Mike LeMaster, Philip Matern, Katie Morrison-Graham, Kristen Oja, Devon Quick, Jon Runyeon, OSU OERU, and OpenStax. *Anatomy and Physiology* 2019; Available from: https://open.oregonstate.education/aandp/chapter/6-3-bone-structure/.
4. Polo-Corrales, L., M. Latorre-Esteves, and J.E. Ramirez-Vick, *Scaffold design for bone regeneration.* J Nanosci Nanotechnol, 2014. **14**(1): p. 15-56.
5. Blumer, M.J.F., *Bone tissue and histological and molecular events during development of the long bones.* Annals of Anatomy - Anatomischer Anzeiger, 2021. **235**: p. 151704.
6. Šromová, V., D. Sobola, and P. Kaspar, *A Brief Review of Bone Cell Function and Importance.* Cells, 2023. **12**(21): p. 2576.
7. Feng, X., *Chemical and Biochemical Basis of Cell-Bone Matrix Interaction in Health and Disease.* Curr Chem Biol, 2009. **3**(2): p. 189-196.
8. Stock, S.R., *The Mineral-Collagen Interface in Bone.* Calcif Tissue Int, 2015. **97**(3): p. 262-80.
9. Yu, L. and M. Wei, *Biomineralization of Collagen-Based Materials for Hard Tissue Repair.* Int J Mol Sci, 2021. **22**(2).
10. Antebi, B., et al., *Biomimetic collagen-hydroxyapatite composite fabricated via a novel perfusion-flow mineralization technique.* Tissue Eng Part C Methods, 2013. **19**(7): p. 487-96.
11. Bose, S., M. Roy, and A. Bandyopadhyay, *Recent advances in bone tissue engineering scaffolds.* Trends in Biotechnology, 2012. **30**(10): p. 546-554.
12. Selim, M., et al., *Innovative designs of 3D scaffolds for bone tissue regeneration: Understanding principles and addressing challenges.* European Polymer Journal, 2024. **215**: p. 113251.
13. DoITPoMS, U.o.C. *Structure of Bone and Implant Materials*. 2004-2025; Available from: https://www.doitpoms.ac.uk/tlplib/bones/structure.php.
14. Wu, A.-M., et al., *Global, regional, and national burden of bone fractures in 204 countries and territories, 1990–2019: a systematic analysis from the Global Burden of Disease Study 2019.* The Lancet Healthy Longevity, 2021. **2**(9): p. e580-e592.

15. ElHawary, H., et al., *Bone Healing and Inflammation: Principles of Fracture and Repair.* Semin Plast Surg, 2021. **35**(3): p. 198-203.
16. Sarkar, S.K. and B.T. Lee, *Hard tissue regeneration using bone substitutes: an update on innovations in materials.* Korean J Intern Med, 2015. **30**(3): p. 279-93.
17. Schemitsch, E.H., *Size Matters: Defining Critical in Bone Defect Size!* Journal of Orthopaedic Trauma, 2017. **31**: p. S20-S22.
18. Azi, M.L., et al., *Autologous bone graft in the treatment of post-traumatic bone defects: a systematic review and meta-analysis.* BMC Musculoskeletal Disorders, 2016. **17**(1): p. 465.
19. Pazhamannil, R.V. and M. Alkhedher, *Advances in additive manufacturing for bone tissue engineering: materials, design strategies, and applications.* Biomedical Materials, 2025. **20**(1): p. 012002.
20. Lutzweiler, G., A. Ndreu Halili, and N. Engin Vrana, *The Overview of Porous, Bioactive Scaffolds as Instructive Biomaterials for Tissue Regeneration and Their Clinical Translation.* Pharmaceutics, 2020. **12**(7): p. 602.
21. Sheikh, Z., et al., *Biodegradable Materials for Bone Repair and Tissue Engineering Applications.* Materials (Basel), 2015. **8**(9): p. 5744-5794.
22. Lee, S.S., et al., *Scaffolds for bone-tissue engineering.* Matter, 2022. **5**(9): p. 2722-2759.
23. Bose, S., M. Roy, and A. Bandyopadhyay, *Recent advances in bone tissue engineering scaffolds.* Trends Biotechnol, 2012. **30**(10): p. 546-54.
24. Khan, W.S., et al., *An osteoconductive, osteoinductive, and osteogenic tissue-engineered product for trauma and orthopaedic surgery: how far are we?* Stem Cells Int, 2012. **2012**: p. 236231.
25. Niu, Y., T. Du, and Y. Liu, *Biomechanical Characteristics and Analysis Approaches of Bone and Bone Substitute Materials.* Journal of Functional Biomaterials, 2023. **14**(4): p. 212.
26. Ghassemi, T., et al., *Current Concepts in Scaffolding for Bone Tissue Engineering.* The Archives of Bone and Joint Surgery, 2018. **6**(2): p. 90-99.
27. Todd, E.A., et al., *Functional Scaffolds for Bone Tissue Regeneration: A Comprehensive Review of Materials, Methods, and Future Directions.* Journal of Functional Biomaterials, 2024. **15**(10): p. 280.
28. Amann, E., et al., *A Graded, Porous Composite of Natural Biopolymers and Octacalcium Phosphate Guides Osteochondral Differentiation of Stem Cells.* Advanced Healthcare Materials, 2021. **10**(6): p. 2001692.
29. Kanwar, S. and S. Vijayavenkataraman, *Design of 3D printed scaffolds for bone tissue engineering: A review.* Bioprinting, 2021. **24**: p. e00167.

30. Fan, J., et al., *A Review of Recent Advances in Natural Polymer-Based Scaffolds for Musculoskeletal Tissue Engineering.* Polymers (Basel), 2022. **14**(10).
31. Guo, L., et al., *The role of natural polymers in bone tissue engineering.* Journal of Controlled Release, 2021. **338**: p. 571-582.
32. Hu, T., et al., *Advances of naturally derived biomedical polymers in tissue engineering.* Frontiers in Chemistry, 2024. **Volume 12 - 2024**.
33. Phutane, P., et al., *Biofunctionalization and Applications of Polymeric Nanofibers in Tissue Engineering and Regenerative Medicine.* Polymers, 2023. **15**(5): p. 1202.
34. Raut, M.P., et al., *Bacterial Cellulose-Based Blends and Composites: Versatile Biomaterials for Tissue Engineering Applications.* International Journal of Molecular Sciences, 2023. **24**(2): p. 986.
35. Avcioglu, N.H., *Bacterial cellulose: recent progress in production and industrial applications.* World Journal of Microbiology and Biotechnology, 2022. **38**(5): p. 86.
36. Manoukian, O.S., et al., *Biomaterials for Tissue Engineering and Regenerative Medicine*, in *Encyclopedia of Biomedical Engineering*, R. Narayan, Editor. 2019, Elsevier: Oxford. p. 462-482.
37. Jiříčková, A., et al., *Synthesis and Applications of Graphene Oxide.* Materials (Basel), 2022. **15**(3).
38. Hummers, W.S., Jr. and R.E. Offeman, *Preparation of Graphitic Oxide.* Journal of the American Chemical Society, 1958. **80**(6): p. 1339-1339.
39. Smith, A.T., et al., *Synthesis, properties, and applications of graphene oxide/reduced graphene oxide and their nanocomposites.* Nano Materials Science, 2019. **1**(1): p. 31-47.
40. Jiříčková, A., et al., *Synthesis and Applications of Graphene Oxide.* Materials, 2022. **15**(3): p. 920.
41. Shaban, N.Z., et al. *Cellulose Acetate Nanofibers: Incorporating Hydroxyapatite (HA), HA/Berberine or HA/Moghat Composites, as Scaffolds to Enhance In Vitro Osteoporotic Bone Regeneration*. Polymers, 2021. **13**, DOI: 10.3390/polym13234140.
42. Kamal, H., F.M. Abd-Elrahim, and S. Lotfy, *Characterization and some properties of cellulose acetate-co-polyethylene oxide blends prepared by the use of gamma irradiation.* Journal of Radiation Research and Applied Sciences, 2014. **7**(2): p. 146-153.
43. Fischer, S., et al., *Properties and Applications of Cellulose Acetate.* Macromolecular Symposia, 2008. **262**(1): p. 89-96.

44. Zhou, K., et al., *Hierarchically Porous Hydroxyapatite Hybrid Scaffold Incorporated with Reduced Graphene Oxide for Rapid Bone Ingrowth and Repair.* ACS Nano, 2019. **13**(8): p. 9595-9606.
45. Ylinen, P., *Applications of coralline hydroxyapatite with bioabsorbable containment and reinforcement as bone graft substitute : An experimental study.* 2006.
46. Ghassemi, T., et al., *Current Concepts in Scaffolding for Bone Tissue Engineering.* Arch Bone Jt Surg, 2018. **6**(2): p. 90-99.
47. Garg, T., et al., *Scaffold: A Novel Carrier for Cell and Drug Delivery.* 2012. **29**(1): p. 1-63.
48. Nga, N.K., T.T.T. Huyen, and T.N. Dung, *Solvent casting-particulate leaching synthesis of a nano-SiO/chitosan composite scaffold for potential use in bone tissue engineering.* Vietnam Journal of Chemistry, 2023. **61**(5): p. 605-611.
49. Afjoul, H., A. Shamloo, and A. Kamali, *Freeze-gelled alginate/gelatin scaffolds for wound healing applications: An in vitro, in vivo study.* Materials Science and Engineering: C, 2020. **113**: p. 110957.
50. N. Musthafa, H.-S., J. Walker, and M. Domagala, *Computational Modelling and Simulation of Scaffolds for Bone Tissue Engineering.* Computation, 2024. **12**(4): p. 74.
51. Zhang, L., et al., *A topology strategy to reduce stress shielding of additively manufactured porous metallic biomaterials.* International Journal of Mechanical Sciences, 2021. **197**: p. 106331.
52. Kelly, C.N., et al., *Fatigue behavior of As-built selective laser melted titanium scaffolds with sheet-based gyroid microarchitecture for bone tissue engineering.* Acta Biomaterialia, 2019. **94**: p. 610-626.
53. Guo, S., et al., *3D-printed laponite bioceramic triply periodic minimal surface scaffolds with excellent bioactivity for bone regeneration.* Ceramics International, 2025. **51**(1): p. 980-990.
54. Baumer, V., et al., *Robocasting of Ceramic Fischer–Koch S Scaffolds for Bone Tissue Engineering.* Journal of Functional Biomaterials, 2023. **14**(5): p. 251.
55. Yang, Y., et al., *Additive manufacturing of bone scaffolds.* IJB, 2018. **5**(1).
56. Boccaccio, A., et al., *Finite element method (FEM), mechanobiology and biomimetic scaffolds in bone tissue engineering.* Int J Biol Sci, 2011. **7**(1): p. 112-32.
57. Patrachari, A.R., J.T. Podichetty, and S.V. Madihally, *Application of computational fluid dynamics in tissue engineering.* Journal of Bioscience and Bioengineering, 2012. **114**(2): p. 123-132.

58. Omar, A.M., et al., *Geometry-Based Computational Fluid Dynamic Model for Predicting the Biological Behavior of Bone Tissue Engineering Scaffolds.* Journal of Functional Biomaterials, 2022. **13**(3): p. 104.
59. Kim, J., et al., *Development of bio-graphite from waste coffee grounds via catalytic graphitization for sustainable Lithium ion batteries anodes.* FlatChem, 2025. **51**: p. 100867.
60. Challa, A.A., et al., *Graphene oxide produced from spent coffee grounds in electrospun cellulose acetate scaffolds for tissue engineering applications.* Materials Today Communications, 2023. **35**: p. 105974.
61. Ullah, M.W., et al., *Advanced biotechnological applications of bacterial nanocellulose-based biopolymer nanohybrids: A review.* Advanced Industrial and Engineering Polymer Research, 2024. **7**(1): p. 100-121.
62. Kalyani, P. and M. Khandelwal, *Modulation of morphology, water uptake/retention, and rheological properties by in-situ modification of bacterial cellulose with the addition of biopolymers.* Cellulose, 2021. **28**(17): p. 11025-11036.
63. Neelima, S., et al., *Highly crystalline bacterial cellulose production by Novacetimonas hansenii strain isolated from rotten fruit.* Materials Letters, 2023. **333**: p. 133622.
64. Challa, A.A., et al., *Bacterial Cellulose/Graphene Oxide/Hydroxyapatite Biocomposite: A Scaffold from Sustainable Sources for Bone Tissue Engineering.* ACS Applied Materials & Interfaces, 2025. **17**(1): p. 572-582.
65. Atykyan, N., V. Revin, and V. Shutova, *Raman and FT-IR Spectroscopy investigation the cellulose structural differences from bacteria Gluconacetobacter sucrofermentans during the different regimes of cultivation on a molasses media.* AMB Express, 2020. **10**(1): p. 84.
66. Amir Faiz, M.S., et al., *Preparation and characterization of graphene oxide from tea waste and it's photocatalytic application of TiO2/graphene nanocomposite.* Materials Research Express, 2020. **7**(1): p. 015613.
67. Thithai, V., et al., *Physicochemical Properties of Activated Carbons Produced from Coffee Waste and Empty Fruit Bunch by Chemical Activation Method.* Energies, 2021. **14**(11): p. 3002.
68. Mahmoudi, E., et al., *Distinguishing characteristics and usability of graphene oxide based on different sources of graphite feedstock.* Journal of Colloid and Interface Science, 2019. **542**: p. 429-440.
69. Mohd Pu'ad, N.A.S., et al., *Syntheses of hydroxyapatite from natural sources.* Heliyon, 2019. **5**(5).

70. Kanjwal, M.A. and A.A. Ghaferi, *Graphene Incorporated Electrospun Nanofiber for Electrochemical Sensing and Biomedical Applications: A Critical Review.* Sensors, 2022. **22**(22): p. 8661.
71. Gabryś, T., et al., *GO-Enabled Bacterial Cellulose Membranes by Multistep, In Situ Loading: Effect of Bacterial Strain and Loading Pattern on Nanocomposite Properties.* Materials, 2023. **16**(3): p. 1296.
72. Torgbo, S. and P. Sukyai, *Biodegradation and thermal stability of bacterial cellulose as biomaterial: The relevance in biomedical applications.* Polymer Degradation and Stability, 2020. **179**: p. 109232.
73. Ielo, I., et al., *Recent Advances in Hydroxyapatite-Based Biocomposites for Bone Tissue Regeneration in Orthopedics.* International Journal of Molecular Sciences, 2022. **23**(17): p. 9721.
74. Shi, H., et al., *Hydroxyapatite Based Materials for Bone Tissue Engineering: A Brief and Comprehensive Introduction.* Crystals, 2021. **11**(2): p. 149.
75. Xing, J. and S. Liu, *Application of loaded graphene oxide biomaterials in the repair and treatment of bone defects.* Bone Joint Res, 2024. **13**(12): p. 725-740.
76. Sabik, A., et al., *Evaluation of PLA gyroid scaffold for long bone fracture treatment: numerical and experimental study.* Journal of the Mechanical Behavior of Biomedical Materials, 2025. **170**: p. 107110.
77. Nazari, Z., B. Ameri, and F. Taheri-Behrooz, *Impact of Voronoi network irregularities and polymer infiltration on the stress intensity factor of 3D-printed bone scaffolds.* Engineering Fracture Mechanics, 2025. **325**: p. 111292.

LIST OF FIGURES

LIST OF TABLES

LIST OF ABBREVIATIONS

BC	Bacterial cellulose
BCC	Body-centered cubic
BMPs	Bone morphogenetic proteins
BTE	Bone tissue engineering
BTR	Bone tissue regeneration
CA	Cellulose acetate
CAD	Computer aided design
CFD	Computational fluid dynamics
CT	Computed tomography
DMAc	Dimethylacetamide
DMEM	Dulbecco's modified eagle medium
ECM	Extracellular matrix
EDX	Energy dispersive x-ray
FBS	Fetal bovine serum
FCC	Face-centered cubic
FEA	Finite element analysis
FTIR	Fourier-transform infrared

FVM	Finite volume method
GO	Graphene oxide
HAp	Hydroxyapatite
HS	Hestrin−Schramm
MRI	Magnetic resonance imaging
MSCs	Mesenchymal stem cells
PBS	Phosphate-buffered saline
PCL	Polycaprolactone
PEG	Polyethylene glycol
PGA	Polyglycolic acid
PLA	Polylactic acid
PLLA	Poly-L-lactic acid
PVDF	Polyvinylidene fluoride
SEM	Scanning electron microscopy
TGA	Thermogravimetric analysis
TGF	Transforming growth factors
TPMS	Triply periodic minimal surfaces
WSS	Wall shear stress
XRD	X-ray diffraction

LIST OF PUBLICATIONS

Publication I

Graphene-Based Carbonaceous Materials: A Sustainable Biomaterial for Biomedical Application. Adam Aberra Challa, Nabanita Saha, and Petr Saha. *Sustainable Green Biomaterials As Drug Delivery Systems*, Springer Nature Switzerland: Cham. p. 165-193 (2025)

Publication II

Graphene oxide produced from spent coffee grounds in electrospun cellulose acetate scaffolds for tissue engineering applications. Adam Aberra Challa, Nabanita Saha, Piotr K. Szewczyk, Joanna E. Karbowniczek, Urszula Stachewicz, Fahanwi Asabuwa Ngwabebhoh, and Petr Saha. *Materials Today Communications*, **35**: p. 105974 (2023)

Publication III

Bacterial Cellulose/Graphene Oxide/Hydroxyapatite Biocomposite: A Scaffold from Sustainable Sources for Bone Tissue Engineering. Adam Aberra Challa, Nabanita Saha, Tanya Zhivkova, Radostina Alexandrova, and Petr Saha. *ACS Applied Materials & Interfaces.* **17**(1): p. 572-582. (2025)

Publication IV (submitted in July 2025)

In-vitro and In-vivo evaluations of bacterial cellulose biocomposite scaffolds for bone tissue engineering applications. Adam Aberra Challa, Nabanita Saha, Tanya Zhivkova, Katerina Todorova, Petar Dimitrov, Radostina Alexandrova, Petr Saha (*Acta Biomaterialia*)

Publication V (under preparation)

Finite element analysis and computational fluid dynamics for Voronoi-based bone scaffold. Adam Aberra Challa, Nabanita Saha, and Petr Saha.

CURRICULUM VITAE

PERSONAL INFORMATION

Name	**Adam Aberra Challa**
Address	J.A. Bati, 5648, Zlin, 76001, Czech Republic
Tel	+420 773 149 874
E-mail	Challa@utb.cz
LinkedIn	linkedin.com/in/adam-aberra
Google Scholar /ResearchGate	Adam Aberra Challa
Nationality	Ethiopian
Date of birth	June 01, 1991

EDUCATION

Ph.D. Education	Ph.D. student in Biomaterials and Bio-composites
Dissertation title	Bio—based Scaffolds for Bone Tissue Regeneration
Duration	*September 2021 – expected September 2025*
Institute	Tomas Bata University in Zlin, Czech Republic
Postgraduate Education	M.Sc. degree in Structural Engineering
Duration	*September 2014 – October 2019*
Institute	Addis Ababa Institute of Technology, Addis Ababa University, Ethiopia
Undergraduate Education	B.Sc. degree in Civil Engineering
Duration	*September 2008 – June 2013*
Institute	Addis Ababa Institute of Technology, Addis Ababa University, Ethiopia

RESEARCH EXPERIENCE

Doctoral Researcher

Tomas Bata University, Center of Polymer Systems, Zin, Czech Republic: *2021–present*

- Synthesized biomaterials including hydroxyapatite, bacterial cellulose, and graphene oxide from sustainable sources
- Conducted several characterizations including SEM, XRD, FTIR, TEM and Rheology procedures
- Conducted materials mechanical testing
- Published research findings in peer-reviewed journals.

Trainee, ERASMUS

Institute of Experimental Morphology, Pathology and Anthropology with Museum, Sofia, Bulgaria: *10 May 2024 – 22 July 2024*

- Conducted in-vitro study and In-vivo testing of biowaste-based scaffolds for bone tissue engineering application

Short-Term Scientific Mission, CONTEXT (CA17107)

Electrospun Fibers Group, AGH University of Science and Technology, Krakow, Poland: *19 Sep 2023 – 18 Oct 2023*

- Fabricated cellulose acetate nanofibers for bone tissue scaffolds using electrospinning
- Performed the characterization and testing of the scaffolds

Trainee, INJECT-BIO (M.ERA.NET)

RTU Rudolfs Cimdins Riga Biomaterials Innovations and Development Centre, Riga, Latvia: *22 Aug – 31 Aug, 2022*

- Analysed bioactive injectable hydrogels
- Performed in-vitro cell studies

Trainee, COST Action (CONTEXT (CA17107))
PRISMA (Emerging Technologies Center0, Prato, Italy**:** *12 Jul – 15 Jul, 2022*

- Attended training on technologies, values and applications of smart textiles

WORK EXPERIENCE

Duration	*June 2015 – August 2021*
Position held	Structural Engineer
Main responsibilities	Design of structures for buildings, supervision of construction sites with projects of the employer, evaluation of building materials and contractual documents
Employer	kenmos Engineering, Addis Ababa, Ethiopia
Duration	*January 2014 – August 2021*
Position held	Lecturer
Main responsibilities	Instruction of students on different courses including structural design, theory of structures and strength of materials, advisement of graduating students in their graduate thesis, advisement of students in their internship work
Employer	Addis Ababa Institute of Technology, Addis Ababa, Ethiopia

PERSONAL SKILLS

Communication Skills	Well-built communication skills through membership and leadership of different organizations including Toastmasters International
Social skills	Good interpersonal skills, ability to easily socialize in a diverse group and good team work skills.

Organisational competences	Proven team management skills developed through participation in various institutions and an association
Computer skills	Capable of operating MS-Office applications, Engineering software - SAP, Ms Project and ETABS, ANSYS and Design software – AutoCAD, Rhinoceros, Blender

PUBLICATIONS

Journal articles [available in Web of Science & Scopus database]

- Challa, A.A., et al., *Bacterial Cellulose/Graphene Oxide/Hydroxyapatite Biocomposite: A Scaffold from Sustainable Sources for Bone Tissue Engineering.* ACS Applied Materials & Interfaces, 2025. **17**(1): p. 572-582. [Q1]
- Challa, A.A., et al., *Graphene oxide produced from spent coffee grounds in electrospun cellulose acetate scaffolds for tissue engineering applications.* Materials Today Communications, 2023. **35**: p. 105974. [Q2]

Book chapter

- Challa, A.A., N. Saha, and P. Saha, *Graphene-Based Carbonaceous Materials: A Sustainable Biomaterial for Biomedical Application*, in *Sustainable Green Biomaterials As Drug Delivery Systems*, R. Malviya and S. Sundram, Editors. 2025, Springer Nature Switzerland: Cham. p. 165-193.

CONFERENCE PRESENTATIONS

SPE MiniTec 2023 conference - New trends in medical plastics
"Biomineralized hydroxyapatite/graphene oxide/bacterial cellulose scaffolds for bone tissue engineering: A green synthesis"

- Zlin, Czech Republic
- *18 Oct 2023 – 19 Oct 2023*

IEEE 12th International Conference "Nanomaterials: Applications & Properties" (IEEE NAP-2022)
"Synthesis and characterization of graphene oxide from residual biomass"

- Krakow, Poland
- *11 Sep 2022 – 16 Sep 2022*

SCHOLARSHIP

Sep 2021 – Present - Ministry of Education, Youth and Sports support of foreign nationals (MSMT-44726/2013)

Adam Aberra Challa, Ph.D.

Bio-based Scaffolds for Bone Tissue Regeneration

Biologické Scaffoldy pro Regeneraci Kostní Tkáně

Doctoral Thesis Summary

Published by: Tomas Bata University in Zlín,

nám. T. G. Masaryka 5555, 760 01 Zlín.

Edition: published electronically

Typesetting by: Adam Aberra Challa

This publication has not undergone any proofreading or editorial review.

Publication year: 2025

First Edition

ISBN 978-80-7678-361-4